JBC Papers in Press. Published on September 20, 2010 as Manuscript M110.166231
The latest version is at http://www.jbc.org/cgi/doi/10.1074/jbc.M110.166231

THE FARNESOID X RECEPTOR REGULATES ADIPOCYTE DIFFERENTIATION AND FUNCTION BY PROMOTING PEROXISOME PROLIFERATOR-ACTIVATED RECEPTOR-γ AND INTERFERING WITH THE WNT/β-CATENIN PATHWAYS

Mouaadh Abdelkarim[1, 2, 3, 4], Sandrine Caron[1, 2, 3, 4], Christian Duhem[1, 2, 3, 4], Janne Prawitt[1, 2, 3, 4] Julie Dumont[1, 2, 3, 4], Anthony Lucas[1,2,3,4], Emmanuel Bouchaert[1, 2, 3, 4], Olivier Briand[1, 2, 3, 4], John Brozek[5], Folkert Kuipers[6], Catherine Fievet[1, 2, 3, 4], Bertrand Cariou[1, 2, 3, 4, 7] and Bart Staels[1, 2, 3, 4].

[1]Univ Lille Nord de France, F-59000, Lille, France, [2]INSERM, UMR1011, F-59019, Lille, France, [3]UDSL, F-59000, Lille, France, [4]Institut Pasteur de Lille, F-59019, Lille, France, [5]Genfit, Loos, France, [6]Center for Liver, Digestive and Metabolic Diseases, Laboratory of Pediatrics, University Medical Center Groningen, Groningen, The Netherlands, [7]Present adress : INSERM U915, IRTUN, l'Institut du Thorax, 8 Quai Moncousu BP70721, 44007 Nantes Cedex 1, France.
Address correspondence to: Bart Staels, UMR1011 INSERM, Institut Pasteur de Lille, 1 rue du Professeur Calmette, BP245, 59019 Lille, France. Phone: 33-3-20-87-73-88; Fax: 33-3-20-87-73-60; Email: Bart.Staels@pasteur-lille.fr

Running title: FXR controls adipose PPARγ responsiveness

The bile acid receptor Farnesoid X Receptor (FXR) is expressed in adipose tissue, but its function remains poorly defined. Peroxisome proliferator-activated receptor-γ (PPARγ) is a master regulator of adipocyte differentiation and function. The aim of this study was to analyze the role of FXR in adipocyte function and to assess whether it modulates PPARγ action. Therefore, we tested the responsiveness of FXR-deficient mice ($FXR^{-/-}$) and cells to the PPARγ activator rosiglitazone. Our results show that genetically obese $FXR^{-/-}$/*ob/ob* mice displayed a resistance to rosiglitazone treatment. *In vitro,* rosiglitazone treatment did not induce normal adipocyte differentiation and lipid droplet formation in $FXR^{-/-}$ mouse embryonic fibroblasts (MEFs) and preadipocytes. Moreover, $FXR^{-/-}$ MEFs displayed both an increased lipolysis and a decreased *de novo* lipogenesis, resulting in reduced intracellular triglyceride content, even upon PPARγ activation. Retroviral-mediated FXR re-expression in $FXR^{-/-}$ MEFs restored the induction of adipogenic marker genes during rosiglitazone-forced adipocyte differentiation. The expression of Wnt/β-catenin pathway and target genes was increased in $FXR^{-/-}$ adipose tissue and MEFs. Moreover, the expression of several endogenous inhibitors of this pathway was decreased early during the adipocyte differentiation of $FXR^{-/-}$ MEFs. These findings demonstrate that FXR regulates adipocyte differentiation and function by regulating two counteracting pathways of adipocyte differentiation, the PPARγ and Wnt/β-catenin pathways.

The nuclear receptor Farnesoid X Receptor (FXR) is a transcription factor which belongs to the nuclear receptor superfamily that is endogenously activated by bile acids (BA) [1]. FXR was initially found to regulate BA metabolism and to protect the liver from the deleterious effect of excessive BA accumulation [2][3][4]. The phenotype of FXR-deficient ($FXR^{-/-}$) mice further established a role for FXR in lipid metabolism [5]. Recently, FXR was shown to be implicated in the control of hepatic glucose metabolism and peripheral insulin sensitivity [6][7][8][9]. FXR modulates the fasting-refeeding transition in mice [8] and genetic murine models of diabetes display an increased FXR expression [10]. While FXR-deficiency was associated with peripheral insulin resistance [6][7], activation of FXR by bile acids [6] or specific synthetic agonists [7][9] conversely improves glucose homeostasis in rodent models of diabetes. Finally, FXR appears to be involved in the regulation of adaptive thermogenesis in response to fasting or cold exposure [11].

The primary role of adipose tissue is to store energy in form of triglycerides (TG) in the adipocytes, which can be liberated as fatty acids upon energy requirement. Adipose tissue is also an endocrine organ secreting hormones involved in metabolic homeostasis [12]. Preadipocyte differentiation into mature adipocytes is a finely tuned process that is regulated by a complex network of transcription factors. In this cascade, the peroxisome proliferator-activated receptor-γ (PPARγ) [13] and CAAT/enhancer-binding protein (C/EBP) α [14] act as key regulators. Early regulators of preadipocyte differentiation are other members of the CAAT/enhancer binding protein family, C/EBPβ and C/EBPδ [15], which induce the expression of PPARγ and C/EBPα [16]. Amongst the extracellular signaling pathways that regulate adipogenesis is the Wnt pathway [17]. The non-canonical and canonical Wnt signaling pathways, being respectively β-catenin-independent and -dependent, are negative regulators of adipogenesis [17]. In the absence of Wnt proteins, β-catenin is localized in the cytoplasm in a protein complex containing Axin and adenomatous polyposis coli (APC) proteins which facilitate β-catenin phosphorylation and its subsequent proteasomal degradation [18]. The binding of Wnt proteins to their receptors Frizzled (FZD) and low-density lipoprotein-receptor related protein-5 or -6 (LRP5/6) leads to β-catenin protein stabilization. Hypophosphorylated β-catenin protein translocates into the nucleus and activates its target genes [19]. The activation of Wnt/β-catenin signalling leads to the repression of adipogenesis by blocking the induction of PPARγ and C/EBPα expression [20]. On the other hand, PPARγ activation leads to proteasomal-dependent β-catenin degradation by stimulating the activity of GSK3β, a β-catenin kinase, and by interacting with phospho-β-catenin itself [20][21][22]. A finely regulated balance between β-catenin activity and PPARγ expression is thus required for proper adipocyte differentiation [23].

We (7) and others (24) have shown that FXR is expressed in adipocyte where it modulates adipocyte differentiation [7][24]. FXR expression was found to be decreased in adipose tissue of mouse models of dietary and genetic obesity [7]. FXR expression is induced during adipocyte differentiation in 3T3-L1 cells and mouse embryonic fibroblasts (MEFs) [7][24]. MEFs isolated from $FXR^{-/-}$ mice ($FXR^{-/-}$ MEFs) display an impaired adipocyte differentiation with a delay in the expression of adipogenic genes and a decreased lipid droplet size [7]. Additionally, FXR activation in 3T3-L1 cells during adipocyte differentiation by specific synthetic agonists increases mRNA expression of adipogenic genes, as well as insulin signaling and insulin-stimulated glucose uptake [7][24].

In the present study, we provide *in vivo* evidence that FXR was necessary for a full response to PPARγ activation. We show that obese $FXR^{-/-}$/*ob/ob* mice displayed an altered response to PPARγ activation by rosiglitazone. Retroviral re-expression of FXR in $FXR^{-/-}$ MEFs restored the adipogenic gene expression program in response to rosiglitazone. The delay in adipogenic differentiation in $FXR^{-/-}$ MEFs was associated with a sustained activation of Wnt/β-catenin signaling. All these results provide evidence for a crucial role of FXR in adipogenesis by promoting the PPARγ pathway and interfering with Wnt/β-catenin signaling.

EXPERIMENTAL PROCEDURES

Animals-Female and male *ob/ob* mice (B6.V-Lepob/J) from Charles River (Saint Aubin les Elseuf, France) were crossed with $FXR^{+/+}$ and $FXR^{-/-}$ C57BL6/J mice to obtain $FXR^{+/+}$/*ob/ob* and $FXR^{-/-}$/*ob/ob* mice. 12 week-old $FXR^{-/-}$ /*ob/ob* female mice and their wild type littermates (n=7/group) were housed on a 12-h light/12-h dark cycle with free access to water and were treated with the PPARγ agonist rosiglitazone (Avandia®, GlaxoSmithKline) (10mg/kg body weight) mixed with control diet (UAR A03, Villemoison/Orge, France) for 21 days.

Isolation and Culture of Mouse Embryonic Fibroblasts (MEFs)-Mouse embryonic fibroblasts (MEFs) were derived from 13.5-day old $FXR^{+/+}$ and $FXR^{-/-}$ embryos

(C57BL6/N) [7]. MEFs were plated in 6-well plates at 300,000 cells/well. Adipocyte differentiation was initiated 2 days after confluence with AmnioMAX-C100 medium (Invitrogen), 7.5% AmnioMAX-C100 supplement, 7.5% fetal bovine serum (FBS), 0.5mM 3-isobutyl-1-methylxanthine (IBMX), 1µM dexamethasone, 5µg/ml insulin. From day 3-8, cells were incubated with AmnioMAX-C100 medium with 5µg/ml insulin and 1µM rosiglitazone. At days 0, 4, and 8, cells were used for lipid metabolism studies (lipolysis, *de novo* lipogenesis and triglyceride content) or lysed and homogenized for RNA isolation or fixed in 4% paraformaldehyde and stained with Oil Red O. All experiments were performed in triplicate.

Preadipocyte Isolation and Culture-Preadipocytes were isolated from inguinal fat pads of 20 week-old $FXR^{-/-}$/*ob/ob* and their $FXR^{+/+}$/*ob*/*ob* littermates. Adipose tissue was isolated, dissociated mechanically and digested in Krebs buffer solution (118mM NaCl, 5mM KCl, 1.25mM $CaCl_2$, 1.2mM KH_2PO_4, 1.2mM $MgSO_4$, 20mM $NaHCO_3$, 2mM Na Pyruvate, 10mM HEPES, 3% BSA, pH7.4) containing 1.5mg/ml collagenase A (Roche Diagnostic GmbH, Germany) for 1.5h in a shaking water bath at 37°C. After digestion, the mature adipocytes were separated from the stroma-vascular cells by centrifugation. The stroma-vascular pellet containing the preadipocytes was treated with erythrocyte lysis solution (154mmol/l NH_4Cl, 10mmol/l $KHCO_3$, 0.1mmol/l EDTA) for 5min at room temperature and centrifuged. The preadipocyte containing pellet was cultured in PromoCell® Preadipocyte Growth Medium (PromoCell® GmbH, Germany) at 37°C in a humidified 95% air and 5% CO_2 incubator. Cultures were grown to confluence (days (-2)). Two days after confluence (day 0), the medium was changed to Preadipocyte Differentiation Medium supplemented with 8µg/ml d-Biotin-4, 0.5µg/ml bovine insulin, 400ng/ml dexamethasone, 44µg/ml IBMX, 9ng/ml L-thyroxine. From day 3-8, the medium was changed to Adipocyte Nutrition Medium and was supplemented with rosiglitazone (1µM). At days 0, 4, and 8, cells were lysed and homogenized for RNA isolation or fixed in 4% paraformaldehyde and stained with Oil Red O.

Measurement of Triglyceride Content-Cellular lipids were extracted with hexane/isopropanol (3:2 vol:vol). Lipids were then dried with nitrogen gas, re-dissolved in isopropanol and quantified using the TG PAP 1000 kit (BioMérieux, Marcy l'Etoile, France).

Lipolysis Assay-Lipolysis experiments were performed at days 4 and 8 of MEF differentiation. Cells were washed with PBS and incubated with 300µl of Incubation Solution (Adipolysis Assay Kit, OB100, Millipore) with 2% BSA or containing 10µM isoproterenol for 3h. Glycerol was measured in the culture supernatant with Free Glycerol Assay Reagent (Adipolysis Assay Kit, OB100, Millipore). Glycerol concentrations were normalized to total cellular protein content. All experiments were performed in triplicate.

De Novo Lipogenesis Assay-De novo lipogenesis was evaluated by measuring incorporation of radiolabeled acetate precursor into total cellular lipids. Cells were washed and incubated with compounds for 48h in culture medium without FBS and with 3mg/ml BSA. Cells were then washed and incubated in Krebs-Ringer buffer for 90min in the presence of 1µCi of [^{14}C]-acetate (Amersham, Saclay, France). MEFs were washed and total cellular lipids were extracted twice with hexane/isopropanol. The pooled organic fractions were transferred to scintillation vials, dried under nitrogen and assessed for radioactivity by liquid scintillation counting. [^{14}C]-acetate incorporation was normalized to total cellular protein content.

Real Time Quantitative Reverse Transcription-PCR-Total RNA was isolated from white adipose tissue using the acid guanidinium thiocyanate/phenol/chloroform method and from MEFs and differentiated preadipocytes using the Trizol reagent (Invitrogen), and subsequently reverse-transcribed using Moloney Murine Leukemia Virus (MMLV) (Applied Biosytems, Paris, France). cDNAs were quantified by quantitative polymerase chain reaction (Quantitative PCR) on a Mx4000 apparatus (Stratagene) using specific primers (Sup. table1). mRNA levels were subsequently normalized to those of

cyclophilin. ΔCt was calculated as the difference between the Ct of the gene of interest and that of cyclophilin.

Plasmid and Retrovirus Infection-The retrovirus was constructed using the FXRα3 mouse cDNA. The sequences of the primers used were: atacgcggatcc*atg*gtgatgagtttcaggg and ctc*tag*accctacacgtcactcagctgcgcata (the initiation (atg) and stop (tag) codons are underlined). The FXR coding sequence was cloned into the mammalian expression vector pBabe-Puro (Invitrogen) in BamHI and SalI sites. Human embryonic kidney 293T modified packaging cells (Ecotropic Phoenix) were cultured in Dulbecco's modified Eagle's medium (DMEM) containing 10% FBS and transiently transfected with a pBabe-puro-FXR chimera or a pBabe-puro vector alone as negative control. 48h after transfection, the viral supernatant was harvested and used to infect the MEFs. Selection of MEFs which had incorporated the retrovirus was done by adding puromycine to the medium for 1 week. FXR expression was measured by quantitative PCR.

Treatment with sFRP1 Recombinant Protein. Recombinant human sFRP1 was purchased from R&D Systems (Minneapolis, MN). $FXR^{-/-}$ MEFs were differentiated in the presence or absence of recombinant sFRP1 (75 nmol/l) added at day 0.

Western Blot-Total cellular MEFs protein was extracted using a RIPA lysis buffer (50mM Tris-HCl, 150mM NaCl, 1.0% (v/v) NP-40, 0.5% (w/v) Sodium Deoxycholate, 1.0mM EDTA, 0.1% (w/v) SDS and 0.01% (w/v) sodium azide, pH:7.4). Protein concentration was determined by the Bradford method (Bio-Rad protein assay). Protein samples were denatured by heating to 90°C in SDS-reducing buffer and resolved by electrophoresis on 10% SDS-polyacrylamide gels. After protein transfer, nitrocellulose membranes were incubated with a mouse monoclonal anti-β-catenin antibody (# 610153, BD Transduction laboratoriesTM) for 3h and HRP-conjugated secondary antibody (DAKO A/S, Denmark) for 1h. Proteins were then visualised by chemiluminescence using an ECL detection kit (Amersham Biosciences, Orsay, France).

Adipocyte Size Determination-Inguinal adipose tissue was fixed in 4% neutral buffered paraformaldehyde, embedded in paraffin, cut into 7-µm sections, and stained with hematoxylin. Cell size was determined using ImageJ software (Freeware; Rasband WS. Image J, US National Institutes of Health, Bethesda, Maryland, http://rsb.info.nih.gov/ij/).

Microarray Analysis-Total RNA was prepared from epididymal adipose tissue of $FXR^{+/+}$ and $FXR^{-/-}$ mice and the subsequent steps were performed as described elsewhere [25]. Affymetrix raw data were normalized using the RMA algorithm to obtain expression values in log2 [26]. Log2-transformed expression values were fitted to a linear model according to Limma package (http://www.bioconductor.orf) methods. A model was established in order to identify probesets significantly differentially expressed between $FXR^{+/+}$ and $FXR^{-/-}$ mice. False discovery rate (FDR) correction was applied to take into account multiple testing hypotheses. Selection of relevant probe sets was based on a mean log2-expression value greater than 6.12 in a least one of the two compared conditions, a p-value < 10^{-5} and an absolute fold change value of 1.5. Function of all clustering of regulated genes was performed by Ingenuity Pathway Analysis (www.ingenuity.com).

Statistical Analysis-Statistical significance was analyzed using the unpaired Student's t test. All values are reported as means ± S.D. Values with $p<0.05$ were considered significant.

RESULTS

FXR-deficiency results in a partial resistance to PPARγ activation in adipose tissue in vivo. To explore whether the FXR and PPARγ pathways interact *in vivo*, genetically obese (*ob/ob*) $FXR^{-/-}$ and $FXR^{+/+}$ mice were treated with rosiglitazone (10mg/kg/bw) for 21 days. As a positive control of *in vivo* PPARγ activation [27], mice from both genotypes displayed a comparable increase of brown adipose tissue mass (Fig.1A), a tissue that does not express FXR [11][28]. As expected [7], adipose tissue of $FXR^{-/-}$ mice contained a larger proportion of small adipocytes (average diameter 78 ± 21 µm) than $FXR^{+/+}$ adipose tissue (average diameter 90 ± 26 µm) (Fig.1B

and Supplementary Table 1). Interestingly, whereas PPARγ activation by rosiglitazone led to the appearance of a sub-population of smaller adipocytes in white adipose tissue of $FXR^{+/+}$ mice, likely due to the induction of preadipocyte recruitment [29], this response was not observed in $FXR^{-/-}$ mice (Fig.1B&C and Supplementary Table 1). Moreover, the induction of some PPARγ-target genes like adiponectin and lipoprotein lipase (LPL) by rosiglitazone was abolished in adipose tissue from $FXR^{-/-}$ compared to $FXR^{+/+}$ mice (Fig.2A). Whereas the induction of other PPARγ-target genes (CD36 and aP2) were also reduced in $FXR^{-/-}$ mice, the expression of adipogenic genes, such as C/EBPα and C/EBPβ, were induced to the same level in both genotypes, and PPARγ expression itself was not modified (Fig.2B). Most interestingly, the induction of genes involved in lipid droplet formation, such as perilipin, ADRP and FSP-27 by rosiglitazone was totally abolished in $FXR^{-/-}$ compared to $FXR^{+/+}$ mice, whereas S3-12 expression was not affected (Fig.2C). These data demonstrate that FXR is necessary to ensure the full response to PPARγ activation in adipose tissue.

FXR-deficiency results in an impaired responsiveness to PPARγ activation in mouse embryonic fibroblasts (MEFs) in vitro. To study whether FXR modulates adipocyte PPARγ responsiveness in a cell-autonomous manner, mouse embryonic fibroblasts (MEFs) were isolated from $FXR^{+/+}$ and $FXR^{-/-}$ embryos and differentiated into adipocytes with or without rosiglitazone and the expression of adipocyte differentiation markers was measured. As expected [7], $FXR^{-/-}$ MEFs were resistant to adipocyte differentiation with a lower expression of C/EBPα, PPARγ and aP2 at day 4 of differentiation in the absence of rosiglitazone (Fig.3). Upon PPARγ activation the induction of C/EBPα, PPARγ and aP2 following rosiglitazone treatment was drastically reduced at day 4, and to a lesser extent at day 8, in $FXR^{-/-}$ compared to $FXR^{+/+}$ MEFs (Fig.3). These results show that $FXR^{-/-}$ MEFs are resistant to PPARγ activation which is unable to induce the complete adipogenic differentiation program in these cells.

$FXR^{-/-}$ MEFs exhibit a reduced lipid storage capacity upon PPARγ activation. The functional consequences of the resistance to PPARγ activation was studied by comparing the phenotype of $FXR^{-/-}$ and $FXR^{+/+}$ MEFs differentiated in the presence of rosiglitazone. The increase in triglyceride (TG) content at day 8 of differentiation was significantly lower in $FXR^{-/-}$ MEFs compared to $FXR^{+/+}$ MEFs (Fig.4A). This reduction in TG content can be the consequence of either an increase in TG degradation (lipolysis) and/or a decrease in TG synthesis (lipogenesis). Therefore, basal and β-adrenergically (isoproterenol)-induced lipolysis were assessed by measuring glycerol release into the cell culture medium. Rosiglitazone-treated $FXR^{-/-}$ MEFs displayed an enhanced lipolysis compared to $FXR^{+/+}$ MEFs under both basal conditions and after β-adrenergic stimulation (Fig.4A) which was statistically significant at day 4 of differentiation. Analysis of [^{14}C]-acetate incorporation demonstrated a significant decrease of fatty acid synthesis (*de novo* lipogenesis) in rosiglitazone-treated $FXR^{-/-}$ compared to $FXR^{+/+}$ MEFs at days 4 and 8 of differentiation (Fig.4A). Moreover, PPARγ activated $FXR^{-/-}$ MEFs also exhibited an abnormal morphology with lipid droplets of smaller size (Fig.4B). Accordingly, rosiglitazone-treated $FXR^{-/-}$ MEFs showed decreased expression of several lipid droplet genes at day 4, such as perilipin, ADRP, S3-12, three members of the PAT protein family [30], and FSP-27 [31], a member of the recently identified CIDE protein family (Fig.4C). While perilipin gene expression did not differ between the two genotypes at day 8, ADRP and S3-12 gene expression was still significantly reduced (Fig.4C). These results indicate that FXR plays a critical role in developing a full lipid storage capacity during adipocyte differentiation by controlling the PPARγ-mediated formation of lipid droplets.

$FXR^{-/-}$ preadipocytes display impaired adipocyte differentiation upon PPARγ activation. To determine whether FXR-deficiency also impairs primary adipocyte differentiation upon PPARγ activation, preadipocytes were isolated from the stromal

fraction of inguinal adipose tissue of $FXR^{-/-}$ /*ob/ob* and $FXR^{+/+}$/*ob/ob* littermates and differentiated into adipocytes in the presence of rosiglitazone. C/EBPβ and C/EBPα mRNA levels were clearly lower at day 4 and 8 of differentiation in $FXR^{-/-}$ compared to $FXR^{+/+}$ cells, whereas the reduction of PPARγ and aP2 expression reached significance only at day 4 (Fig.5A). As in differentiated MEFs, 8-day-differentiated rosiglitazone-treated $FXR^{-/-}$ adipocytes exhibited an abnormal morphology with smaller lipid droplets compared to $FXR^{+/+}$ cells (Fig.5B). This phenotype was associated with a transiently reduced expression of the perilipin and FSP-27 genes at day 4, while ADRP and S3-12 gene expression was not affected (Fig.5C). Surprisingly, FSP-27 mRNA levels were found to be increased at day 8 in $FXR^{-/-}$ adipocytes. Altogether, these results show that $FXR^{-/-}$ preadipocytes display altered adipocyte differentiation even when PPARγ is activated.

Re-introduction of FXR in $FXR^{-/-}$ MEFs restores the expression of adipogenic and lipid droplet genes and increases the number of differentiated adipocyte clusters. To determine whether the altered adipocyte differentiation observed in rosiglitazone-treated $FXR^{-/-}$ MEFs was strictly FXR-dependent, FXR was exogenously (re-)expressed in $FXR^{-/-}$ and $FXR^{+/+}$ MEFs using a retrovirus encoding FXRα3, which, together with FXRα4, is expressed in MEF cells (data not shown). Infected cells were subsequently subjected to adipogenic differentiation in the presence of rosiglitazone. Retroviral infection led to a pronounced mRNA expression of FXRα3 in $FXR^{-/-}$ MEFs during adipocyte differentiation, with a 3-fold higher expression at day 8 compared to $FXR^{+/+}$ MEFs infected with empty retrovirus *(data not shown)*. Importantly, re-introduction of FXR resulted in an increased number of differentiated adipocyte clusters (Fig.6A) and a restoration of PPARγ and aP2 expression at day 8, whereas neither the expression of C/EBPβ nor C/EBPα was affected in $FXR^{-/-}$ MEFs (Fig.6B). Moreover, the expression of all lipid droplet genes was significantly increased at day 8 (Fig.6C). Thus, re-expression of FXR in $FXR^{-/-}$ MEFs restores the capacity of MEFs to differentiate into adipocytes upon rosiglitazone treatment.

FXR-deficiency results in a dysregulation of the Wnt/β-catenin pathway in adipose tissue and adipocytes. To unravel the mechanisms underlying the impaired adipocyte differentiation linked to FXR-deficiency, a microarray analysis was performed in white adipose tissue from $FXR^{-/-}$ versus $FXR^{+/+}$ mice to identify pathways with altered expression (*data not shown*). One of those identified is the Wnt/β-catenin signaling pathway known to inhibit adipocyte differentiation at least in part by inhibiting PPARγ activity [19]. Indeed, mRNA levels of β-catenin were increased in adipose tissue of $FXR^{-/-}$ vs $FXR^{+/+}$ obese mice (Fig.7A). In accordance with an increased Wnt/β-catenin signaling, mRNA levels of LRP5 and Axin2 [18], both target genes and components of the Wnt/β-catenin pathway, and the target genes cyclin D1 and c-Myc [32][33], were higher in adipose tissue of $FXR^{-/-}$ compared to $FXR^{+/+}$ mice (Fig.7A).

The expression of regulators and components of the Wnt/β-catenin pathway was also analyzed during the differentiation of $FXR^{+/+}$ and $FXR^{-/-}$ MEFs into adipocytes. Interestingly, the expression of the secreted frizzled-related proteins (sFRP) 1 and 5, negative regulators of the Wnt pathway, was lower in $FXR^{-/-}$ MEFs during early adipocyte differentiation, at day 2 and day 1 respectively (Fig.7B). In parallel, western blot analysis showed that β-catenin protein expression was higher in $FXR^{-/-}$ MEFs with a peak at day 4 compared to $FXR^{+/+}$ MEFs (Fig.7C). In accordance with an increased Wnt/β-catenin signaling, the expression of LRP5, Axin2, cyclin D1 and c-Myc, four target genes of this pathway, was increased in $FXR^{-/-}$ compared to $FXR^{+/+}$ MEFs (Fig.7D). Moreover, restoration of FXR expression in $FXR^{-/-}$ MEFs using the FXRα3 encoding retrovirus resulted in a decrease of β-catenin protein expression (Fig. 7E) along with the improvement of adipocyte differentiation (Fig.6B). Moreover, mRNA expression of the Wnt/β-catenin pathway genes c-Myc, Axin2 and LRP5 decreased upon FXR reintroduction in $FXR^{-/-}$ MEFs (Fig.7E).

To further assess whether the anti-adipogenic effect of FXR-deficiency is mediated by the activation of the Wnt/β-catenin signaling pathway, we investigated whether the secreted Wnt antagonist sFRP1 could reverse this effect. The elevated β-catenin protein expression in $FXR^{-/-}$ compared to $FXR^{+/+}$ MEFs was reduced upon incubation with recombinant sFRP1 protein (Fig.8A). Concomitantly, sFRP1 treatment of $FXR^{-/-}$ MEFs increased the expression of adipogenic markers, such as PPARγ and aP2 (Fig.8B).

These results demonstrate that the Wnt/β-catenin pathway, which inhibits adipocyte differentiation and PPARγ function, is activated in FXR-deficient adipocytes *in vivo* and *in vitro* and that restoration of FXR expression inhibits the Wnt signaling pathway.

DISCUSSION

The results of this study identify a role for the nuclear receptor FXR as a modulator of the PPARγ and Wnt signaling pathways in adipocyte differentiation. $FXR^{-/-}$ mice displayed an impaired response to PPARγ activation and $FXR^{-/-}$ MEFs were resistant to the induction of adipogenic differentiation by PPARγ activation. Our results show that lipid storage is impaired in $FXR^{-/-}$ MEFs even after PPARγ activation due to decreased *de novo* lipogenesis and increased lipolysis. Microarray analysis of adipose tissue from $FXR^{+/+}$ and $FXR^{-/-}$ mice allowed us to identify that FXR-deficiency alters mRNA expression of genes implicated in the Wnt/β-catenin signaling pathway. $FXR^{-/-}$ adipose tissue and $FXR^{-/-}$ MEFs exhibited an over-activation of the Wnt/β-catenin signaling pathway, an inhibitor of adipocyte differentiation and PPARγ function. These results demonstrate that FXR is critical for full adipocyte differentiation by promoting PPARγ activation and interfering with the Wnt/β-catenin signaling pathways.

Our study shows that FXR-deficiency led to impaired adipocyte differentiation of MEFs, as well as preadipocytes isolated from the stromal fraction of $FXR^{-/-}$ adipose tissue, with a clear alteration of lipid droplet gene expression after differentiation in the presence of rosiglitazone. This alteration of mRNA expression in $FXR^{-/-}$ cells was already detectable at day 2 and 4, while the functional consequences reflected in lipid droplet morphology were observed later at day 8 of differentiation. This alteration of adipocyte differentiation induced by rosiglitazone was strictly FXR-dependent since FXR re-introduction improved differentiation of $FXR^{-/-}$ MEFs with an increased expression of adipogenic markers, such as PPARγ and aP2, and an increased number of differentiated cell clusters. Intriguingly, C/EBPα and C/EBPβ mRNA expression was not restored. We have currently no explanation for the lack of response of these two genes.

Rosiglitazone-treated $FXR^{-/-}$ MEFs displayed an alteration of triglyceride storage that was correlated with a combination of a decrease of *de novo* lipogenesis and an increase of lipolysis. In parallel, the expression of lipogenic genes was decreased in $FXR^{-/-}$ MEFs (*data not shown*). This result is in agreement with those obtained in the 3T3-L1 cell line showing an increase of lipogenic gene expression after treatment with FXR agonists [24].

$FXR^{-/-}$ MEFs exhibited an increase of both basal and β-adrenergically-induced lipolysis. However, the extent of β-adrenergically-mediated induction was similar between $FXR^{-/-}$ and $FXR^{+/+}$ MEFs suggesting that downstream pathways are not influenced by FXR. However, the expression of lipid droplet genes such as perilipin, ADRP, S3-12 and FSP-27, which play a role in lipid droplet formation and lipolysis, is altered even after PPARγ activation. Since, $FXR^{-/-}$ MEFs and preadipocytes present a decreased lipid droplet size, it would be interesting to determine the localisation of the ATGL and HSL proteins before and after β-adrenergic stimulation. Indeed, a recent study proposes that these two enzymes are preferentially associated with small lipid droplets [34], and thus could contribute to the increase of lipolysis in $FXR^{-/-}$ adipocytes.

Microarray analysis of white adipose tissue of $FXR^{+/+}$ and $FXR^{-/-}$ mice showed that FXR-deficiency is associated with impaired expression of regulators and components of the Wnt/β-catenin signaling pathway [35]. Interestingly the expression of sFRP5, an

inhibitor of the Wnt/β-catenin signaling pathway, was down-regulated *in vivo* (*data not shown*) and *in vitro* in $FXR^{-/-}$ MEFs. Conversely, β-catenin, a gene implicated in inhibition of adipocyte differentiation and adipose tissue formation [35][36][37], was up-regulated in adipose tissue of $FXR^{-/-}$ mice. This observation is consistent with studies showing that there is an increase of β-catenin in the intestine of $FXR^{-/-}$ mice [38].

sFRP5 mRNA levels correlate with adiposity [39]. Thus, the observed decrease of sFRP5 mRNA expression is in agreement with the description of lower adipose tissue mass in $FXR^{-/-}$ mice [7]. Moreover, the expression of sFRP1, which, when over-expressed, induces spontaneous adipocyte differentiation [40], was decreased in $FXR^{-/-}$ MEFs. mRNA levels of sFRP1 and sFRP5 were decreased respectively at day 2 and day 1 of MEFs differentiation, which correlates with the increased β-catenin protein levels especially at day 4 of $FXR^{-/-}$ MEF differentiation. Moreover, incubation of $FXR^{-/-}$ MEFs with sFRP1 decreased β-catenin protein and increased expression of adipogenic genes. These results show that FXR acts at an early stage of the adipogenic program, at least in part by controlling the expression of negative regulators of Wnt/β-catenin signaling pathway.

Several lines of evidence indicate that the Wnt/β-catenin signaling pathway is increased in $FXR^{-/-}$ adipose tissue and MEF cells. The expression of the receptor LRP5, the regulator of β-catenin stability and phosphorylation Axin2, and the target genes of the Wnt/β-catenin signaling pathway cyclin D1 and c-Myc, were up-regulated in the absence of FXR. Cyclin D1 and c-Myc both inhibit adipocyte differentiation by decreasing PPARγ activity through histone deacetylase recruitment on the promoter of its target genes [32] and by suppressing C/EBPα and p21 gene expression [41]. These results suggest that FXR interferes with the activation of the Wnt/β-catenin signaling pathway to promote adipocyte differentiation. This interference could be mediated by a decrease of β-catenin protein stability *via* a feedback regulation affecting the expression and protein level of Axin2 or LRP5 or *via* the induction of GSK3β, the kinase that phosphorylates the β-catenin protein.

Another argument for the modulation of the Wnt/β-catenin signaling pathway is the observation that FXR-deficiency results in an impaired responsiveness to PPARγ activation *in vitro* and *in vivo*. First, FXR-deficiency altered PPARγ expression in MEFs and FXR re-introduction in $FXR^{-/-}$ MEFs increased mRNA expression of PPARγ. Moreover, $FXR^{-/-}$ MEFs displayed a resistance to the induction of adipocyte differentiation by rosiglitazone treatment. In the same line, $FXR^{-/-}$/*ob*/*ob* mice exhibited an impaired responsiveness to PPARγ activation reflected by altered expression of several PPARγ target genes, including lipid droplet genes. These results further corroborate the existence of a cross-talk between FXR and PPARγ activities, as has been proposed in hepatocytes where FXR increases PPARγ expression, thereby regulating the antifibrotic activity of FXR in rodent liver [42].

In summary, FXR is necessary for a proper response to PPARγ activation, suggesting a cross-talk between FXR and PPARγ. Moreover, FXR contributes to the induction of adipocyte differentiation by interfering with the Wnt/β-catenin signaling pathway. These results identify a critical role for FXR in adipose tissue to ensure the accurate and complete course of adipocyte differentiation.

REFERENCES

1. Lefebvre P, Cariou B, Lien F, Kuipers F & Staels B.(2009) *Physiol. Rev.* **89**: 147-191
2. Makishima M, Okamoto AY, Repa JJ, Tu H, Learned RM, Luk A, Hull MV, Lustig KD, Mangelsdorf DJ & Shan B.(1999) *Science* **284**: 1362-1365
3. Wang H, Chen J, Hollister K, Sowers LC & Forman BM.(1999) *Mol. Cell* **3**: 543-553

4. Parks DJ, Blanchard SG, Bledsoe RK, Chandra G, Consler TG, Kliewer SA, Stimmel JB, Willson TM, Zavacki AM, Moore DD & Lehmann JM.(1999) *Science* **284**: 1365-1368
5. Sinal CJ, Tohkin M, Miyata M, Ward JM, Lambert G & Gonzalez FJ.(2000) *Cell* **102**: 731-744
6. Ma K, Saha PK, Chan L & Moore DD.(2006) *J. Clin. Invest.* **116**: 1102-1109
7. Cariou B, van Harmelen K, Duran-Sandoval D, van Dijk TH, Grefhorst A, Abdelkarim M, Caron S, Torpier G, Fruchart J, Gonzalez FJ, Kuipers F & Staels B.(2006) *J. Biol. Chem.* **281**: 11039-11049
8. Duran-Sandoval D, Cariou B, Percevault F, Hennuyer N, Grefhorst A, van Dijk TH, Gonzalez FJ, Fruchart J, Kuipers F & Staels B.(2005) *J. Biol. Chem.* **280**: 29971-29979
9. Zhang Y, Lee FY, Barrera G, Lee H, Vales C, Gonzalez FJ, Willson TM & Edwards PA.(2006) *Proc. Natl. Acad. Sci. U.S.A.* **103**: 1006-1011
10. Duran-Sandoval D, Mautino G, Martin G, Percevault F, Barbier O, Fruchart J, Kuipers F & Staels B.(2004) *Diabetes* **53**: 890-898
11. Cariou B, Bouchaert E, Abdelkarim M, Dumont J, Caron S, Fruchart J, Burcelin R, Kuipers F & Staels B.(2007) *FEBS Lett.* **581**: 5191-5198
12. Halberg N, Wernstedt-Asterholm I & Scherer PE.(2008) *Endocrinol. Metab. Clin. North Am.* **37**: 753-68, x-xi
13. Tontonoz P, Hu E & Spiegelman BM.(1994) *Cell* **79**: 1147-1156
14. Lin FT & Lane MD.(1994) *Proc. Natl. Acad. Sci. U.S.A.* **91**: 8757-8761
15. Wu Z, Bucher NL & Farmer SR.(1996) *Mol. Cell. Biol.* **16**: 4128-4136
16. Lefterova MI & Lazar MA.(2009) *Trends Endocrinol. Metab.* **20**: 107-114
17. Christodoulides C, Lagathu C, Sethi JK & Vidal-Puig A.(2009) *Trends Endocrinol. Metab.* **20**: 16-24
18. Logan CY & Nusse R.(2004) *Annu. Rev. Cell Dev. Biol.* **20**: 781-810
19. Angers S & Moon RT.(2009) *Nat. Rev. Mol. Cell Biol.* **10**: 468-477
20. Liu J & Farmer SR.(2004) *J. Biol. Chem.* **279**: 45020-45027
21. Sharma C, Pradeep A, Wong L, Rana A & Rana B.(2004) *J. Biol. Chem.* **279**: 35583-35594
22. Farmer SR.(2005) *Int J Obes (Lond)* **29 Suppl 1**: S13-6
23. Moldes M, Zuo Y, Morrison RF, Silva D, Park B, Liu J & Farmer SR.(2003) *Biochem. J.* **376**: 607-613
24. Rizzo G, Disante M, Mencarelli A, Renga B, Gioiello A, Pellicciari R & Fiorucci S.(2006) *Mol. Pharmacol.* **70**: 1164-1173
25. Slonim DK, Koide K, Johnson KL, Tantravahi U, Cowan JM, Jarrah Z & Bianchi DW.(2009) *Proc. Natl. Acad. Sci. U.S.A.* **106**: 9425-9429
26. Irizarry RA, Bolstad BM, Collin F, Cope LM, Hobbs B & Speed TP.(2003) *Nucleic Acids Res.* **31**: e15
27. Lazarenko OP, Rzonca SO, Hogue WR, Swain FL, Suva LJ & Lecka-Czernik B.(2007) *Endocrinology* **148**: 2669-2680
28. Watanabe M, Houten SM, Mataki C, Christoffolete MA, Kim BW, Sato H, Messaddeq N, Harney JW, Ezaki O, Kodama T, Schoonjans K, Bianco AC & Auwerx J.(2006) *Nature* **439**: 484-489
29. Yamauchi T, Kamon J, Waki H, Terauchi Y, Kubota N, Hara K, Mori Y, Ide T, Murakami K, Tsuboyama-Kasaoka N, Ezaki O, Akanuma Y, Gavrilova O, Vinson C, Reitman ML, Kagechika H, Shudo K, Yoda M, Nakano Y, Tobe K, Nagai R, Kimura S, Tomita M, Froguel P & Kadowaki T.(2001) *Nat. Med.* **7**: 941-946
30. Londos C, Brasaemle DL, Schultz CJ, Segrest JP & Kimmel AR.(1999) *Semin. Cell Dev. Biol.* **10**: 51-58
31. Puri V, Konda S, Ranjit S, Aouadi M, Chawla A, Chouinard M, Chakladar A & Czech MP.(2007) *J. Biol. Chem.* **282**: 34213-34218

32. Fu M, Rao M, Bouras T, Wang C, Wu K, Zhang X, Li Z, Yao T & Pestell RG.(2005) *J. Biol. Chem.* **280**: 16934-16941
33. He TC, Sparks AB, Rago C, Hermeking H, Zawel L, da Costa LT, Morin PJ, Vogelstein B & Kinzler KW.(1998) *Science* **281**: 1509-1512
34. Bezaire V, Mairal A, Ribet C, Lefort C, Girousse A, Jocken J, Laurencikiene J, Anesia R, Rodriguez A, Ryden M, Stenson BM, Dani C, Ailhaud G, Arner P & Langin D.(2009) *J. Biol. Chem.* **284**: 18282-18291
35. Kennell JA & MacDougald OA.(2005) J. Biol. Chem. *280: 24004-24***010**
36. Bennett CN, Ross SE, Longo KA, Bajnok L, Hemati N, Johnson KW, Harrison SD & MacDougald OA.(2002) J. Biol. Chem. *277: 30998-31***004**
37. Ross SE, Hemati N, Longo KA, Bennett CN, Lucas PC, Erickson RL & MacDougald OA.(2000) Science 289: *950-953*
38. Modica S, Murzilli S, Salvatore L, Schmidt DR & Moschetta A.(2008) Cancer Res. 6*8: 9589-9594*
39. Lagathu C, Christodoulides C, Virtue S, Cawthorn WP, Franzin C, Kimber WA, Nora ED, Campbell M, Medina-Gomez G, Cheyette BNR, Vidal-Puig AJ & Sethi JK.(2009) Diabetes 58: *609-619*
40. Bhat RA, Stauffer B, Komm BS & Bodine PVN.(2004) Protein Expr. *Purif. 37: 327-335*
41. Freytag SO & Geddes TJ.(1992) Science 256: *379-382*
42. Fiorucci S, Rizzo G, Antonelli E, Renga B, Mencarelli A, Riccardi L, Morelli A, Pruzanski M & Pellicciari R.(2005) J. Pharmacol. *Exp. Ther. 315: 58-68*

ACKNOWLEDGEMENTS

This work was supported by the European Union Grant HEPADIP 018734, COST Action BM0602 and Agence Nationale de la Recherche (ANR) Grant A05056GS. M. Abdelkarim was supported by the Fondation pour la Recherche Médicale (FRM).

FIGURE LEGENDS

Figure 1. **Obese FXR$^{-/-}$/*ob/ob* mice are resistant to the effects of PPARγ activation on adipocyte recruitment. A.** Increase of brown adipose tissue (BAT) mass in FXR$^{-/-}$ and FXR$^{+/+}$/*ob*/*ob* mice after rosiglitazone (RSG) treatment. **B.** Adipocyte size distribution in adipose tissue of FXR$^{-/-}$ and FXR$^{+/+}$/*ob*/*ob* mice treated or not with RSG. 200 adipocytes were studied per section. Adipocyte size was measured using ImageJ. **C.** Morphology of white adipocytes of FXR$^{-/-}$ and FXR$^{+/+}$/*ob*/*ob* mice (n=3/group) treated with RSG (10mg/kg). Small adipocytes recruited after RSG treatment are indicated by the arrow.

Figure 2**. FXR-deficiency alters the expression profile of white adipose tissue genes following rosiglitazone treatment**. mRNA expression of PPARγ target genes (**A**), adipogenic transcription factor genes (**B**) and lipid droplet genes (**C**) in white adipose tissue of FXR$^{-/-}$ and FXR$^{+/+}$/*ob*/*ob* mice after rosiglitazone treatment. mRNA levels were measured by quantitative PCR. Values are normalized to the expression of cyclophilin and are expressed relative to control FXR$^{+/+}$ mice. The results are presented as means ± S.D.

Figure 3. **FXR$^{-/-}$ MEFs are resistant to PPARγ activation**. mRNA levels of adipogenic genes of 4- and 8-day-differentiated FXR$^{-/-}$ and FXR$^{+/+}$ MEFs in the presence or absence of 1 µM rosiglitazone (RSG) were measured by quantitative PCR. Values are normalized to the expression of cyclophilin and are expressed relative to those at day 0, which are arbitrarily set to 1. These results are representative of three experiments and are presented as means ± S.D.

Figure 4. **FXR-deficiency alters triglyceride storage, lipolysis, *de novo* lipogenesis and the expression of lipid droplet genes in MEFs during differentiation to adipocytes**. **A**.

Triglyceride (TG) content in $FXR^{-/-}$ and $FXR^{+/+}$ MEFs at day 0, 4 and 8 of differentiation treated with 1 µM rosiglitazone; lipolysis was measured in $FXR^{-/-}$ and $FXR^{+/+}$ MEFs at day 0, 4 and 8 as glycerol release under basal and stimulated (isoproterenol: ISO) conditions*; de novo* lipogenesis in $FXR^{-/-}$ and $FXR^{+/+}$ MEFs at day 0, 4 and 8 of differentiation. The results are representative of three experiments and are presented as means ± S.D. **B**. Quantification of the lipid droplet size of 8-day-differentiated $FXR^{-/-}$ and $FXR^{+/+}$ MEFs. **C**. mRNA expression of genes coding for lipid droplet proteins in $FXR^{-/-}$ and $FXR^{+/+}$ MEFs during differentiation measured by quantitative PCR. Values are normalized to the expression of cyclophilin and are expressed relative to those at day 0, which are arbitrarily set to 1. The results are representative of three experiments and are presented as means ± S.D.

Figure 5. **FXR-deficiency impairs PPARγ-induced differentiation and lipid droplet formation of primary preadipocytes. A**, **C**. Expression of adipogenic marker (A) and lipid droplet protein (C) genes in $FXR^{-/-}$ compared to $FXR^{+/+}$ preadipocytes treated with 1 µM rosiglitazone. Preadipocytes were isolated from white adipose tissue of obese $FXR^{-/-}$/*ob*/*ob* and $FXR^{+/+}$/*ob/ob* mice. mRNA levels were measured by quantitative PCR. Values (± SD) are normalized to the expression of cyclophilin and are expressed relative to those at day 0, which are arbitrarily set to 1. **B.** Smaller size of lipid droplets in $FXR^{-/-}$ compared to $FXR^{+/+}$ preadipocytes. Representative Oil Red O staining of $FXR^{-/-}$ and $FXR^{+/+}$ preadipocytes at day 0 and 8 of differentiation (20x magnification).

Figure 6. **Re-expression of FXR reverses the impaired adipocyte differentiation of rosiglitazone-treated $FXR^{-/-}$ MEFs.** $FXR^{-/-}$ MEFs were infected with a retrovirus coding for FXRα3 or the empty vector, subjected to adipogenic differentiation and treated with 1 µM rosiglitazone. **A.** Increased number of differentiated cell clusters after FXR retroviral infection of rosiglitazone-treated $FXR^{-/-}$ MEFs. Representative Oil Red O staining of $FXR^{-/-}$ and $FXR^{+/+}$ MEFs at day 8 of differentiation (20x magnification). **B, C.** mRNA levels of adipogenic markers (**B**) and lipid droplet protein (**C**) genes in empty retrovirus- and FXR retrovirus-infected rosiglitazone-treated $FXR^{-/-}$ MEFs measured by quantitative PCR. Empty retrovirus transfected $FXR^{+/+}$ MEFs were used as reference. Values are normalized to cyclophilin mRNA and are expressed relative to those at day 0, which are arbitrarily set to 1. The results are representative of three experiments and are presented as means ± S.D.

Figure 7. **Upregulation of the Wnt/β-catenin signaling pathway in adipose tissue of $FXR^{-/-}$ /*ob*/*ob* mice and $FXR^{-/-}$ MEFs. A**. mRNA expression of β-catenin, LRP5, c-Myc, Axin2 and Cyclin D1 in inguinal adipose tissue of $FXR^{-/-}$ and $FXR^{+/+}$/*ob*/*ob* mice. mRNA levels were measured by quantitative PCR. Values are normalized to the expression of cyclophilin and are expressed relative to $FXR^{+/+}$ mice, which are arbitrarily set to 1. The results are presented as means ± S.D. **B**. mRNA expression of sFRP1 and sFRP5 during differentiation of $FXR^{-/-}$ and $FXR^{+/+}$ MEFs treated with 1 µM rosiglitazone. **C.** β-catenin protein levels during $FXR^{-/-}$ and $FXR^{+/+}$ MEF differentiation. **D.** mRNA levels of Wnt/β-catenin target genes during differentiation of $FXR^{-/-}$ and $FXR^{+/+}$ MEFs. **E.** (top) β-catenin protein levels, (bottom) mRNA levels of c-Myc, Axin2 and LRP5 in $FXR^{+/+}$ and $FXR^{-/-}$ MEFs transfected for 2 days with empty of FXR retrovirus as indicated. mRNA levels were measured by quantitative PCR. Values are normalized to the expression of cyclophilin and are expressed relative to those at day 0, which are arbitrarily set to 1. The results are representative of two experiments and are presented as means ± S.D.

Figure 8. **Secreted Frizzled-Related Protein 1 (sFRP1) reduces β-catenin protein (A) and increases PPARγ and aP2 gene expression in $FXR^{-/-}$ MEFs**. $FXR^{-/-}$ MEFs were differentiated in the presence or absence of recombinant sFRP1 (75 nmol/l). **A**. β-catenin protein levels. **B**. mRNA levels of adipogenic genes measured by quantitative PCR. Values are normalized to the

expression of cyclophilin and are expressed relative to those in $FXR^{+/+}$ MEFs, which are arbitrarily set to 1. These results are presented as means ± S.D.

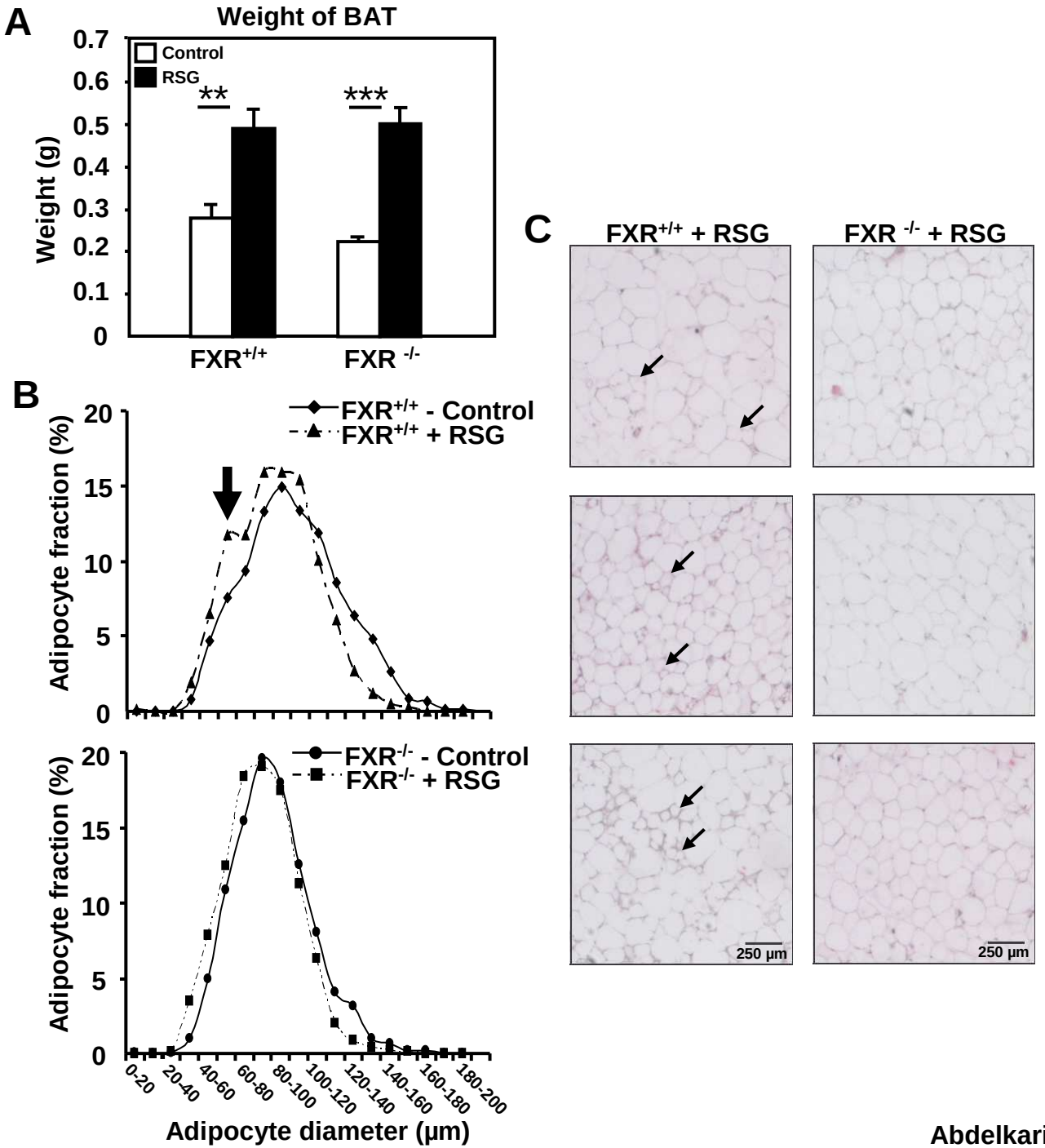

Abdelkarim M et *al*.. Figure 1

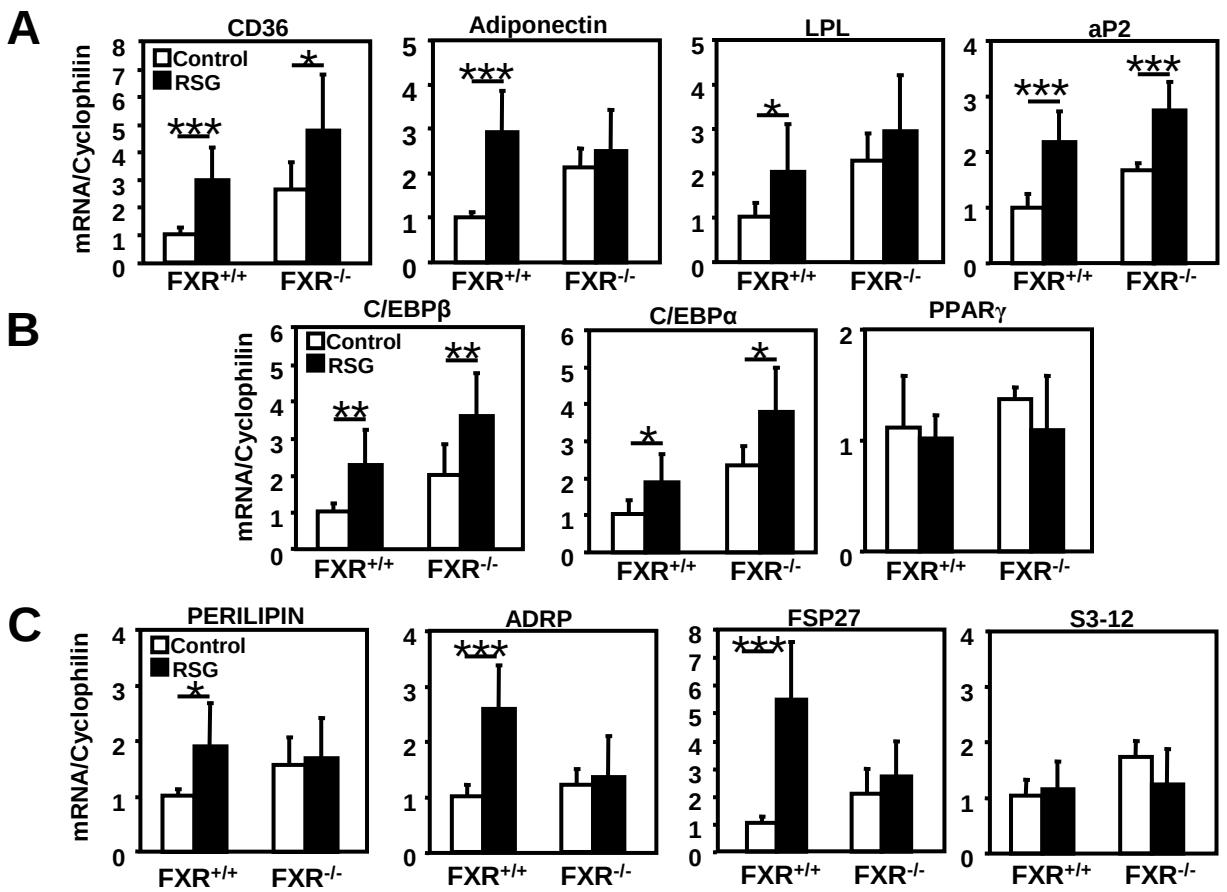

Abdelkarim M et *al*.. Figure 2

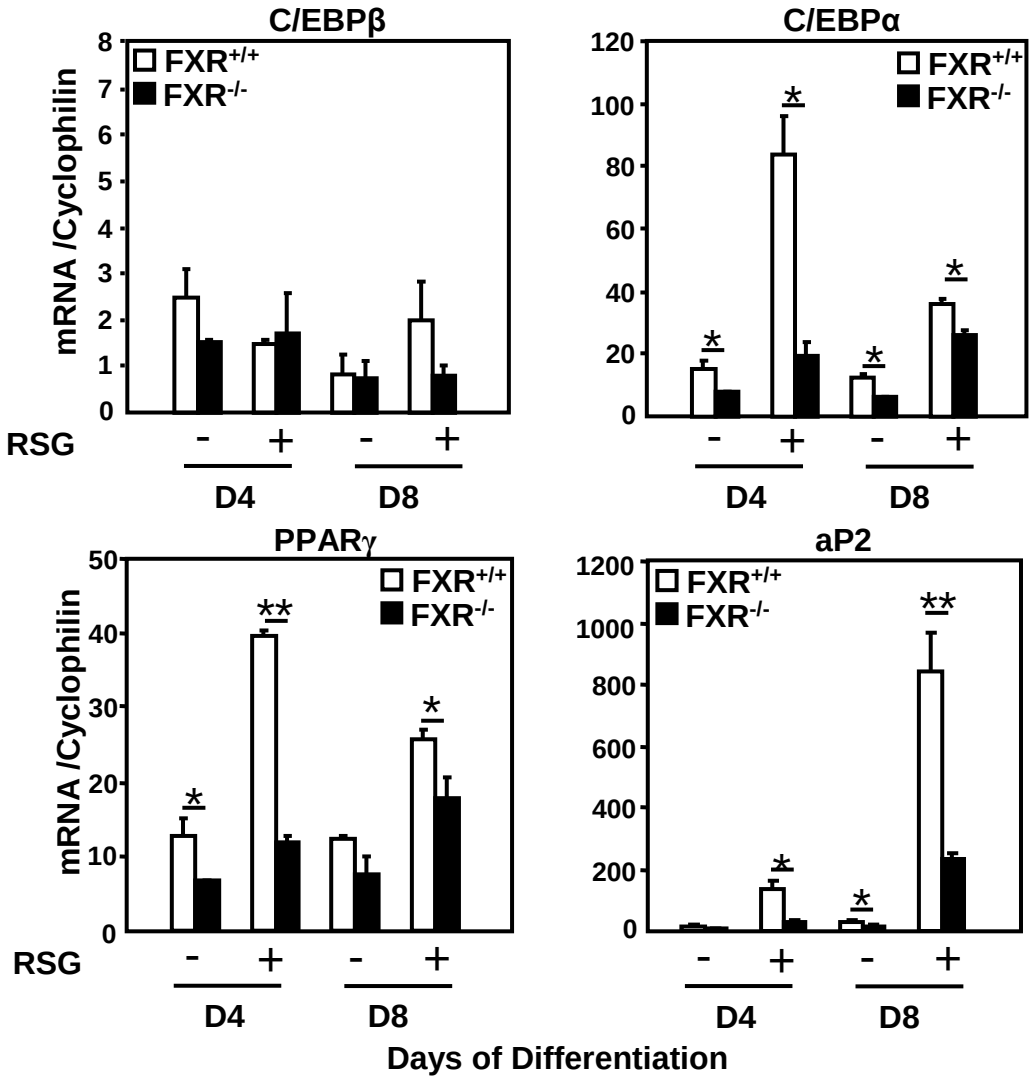

Abdelkarim M et *al*.. Figure 3

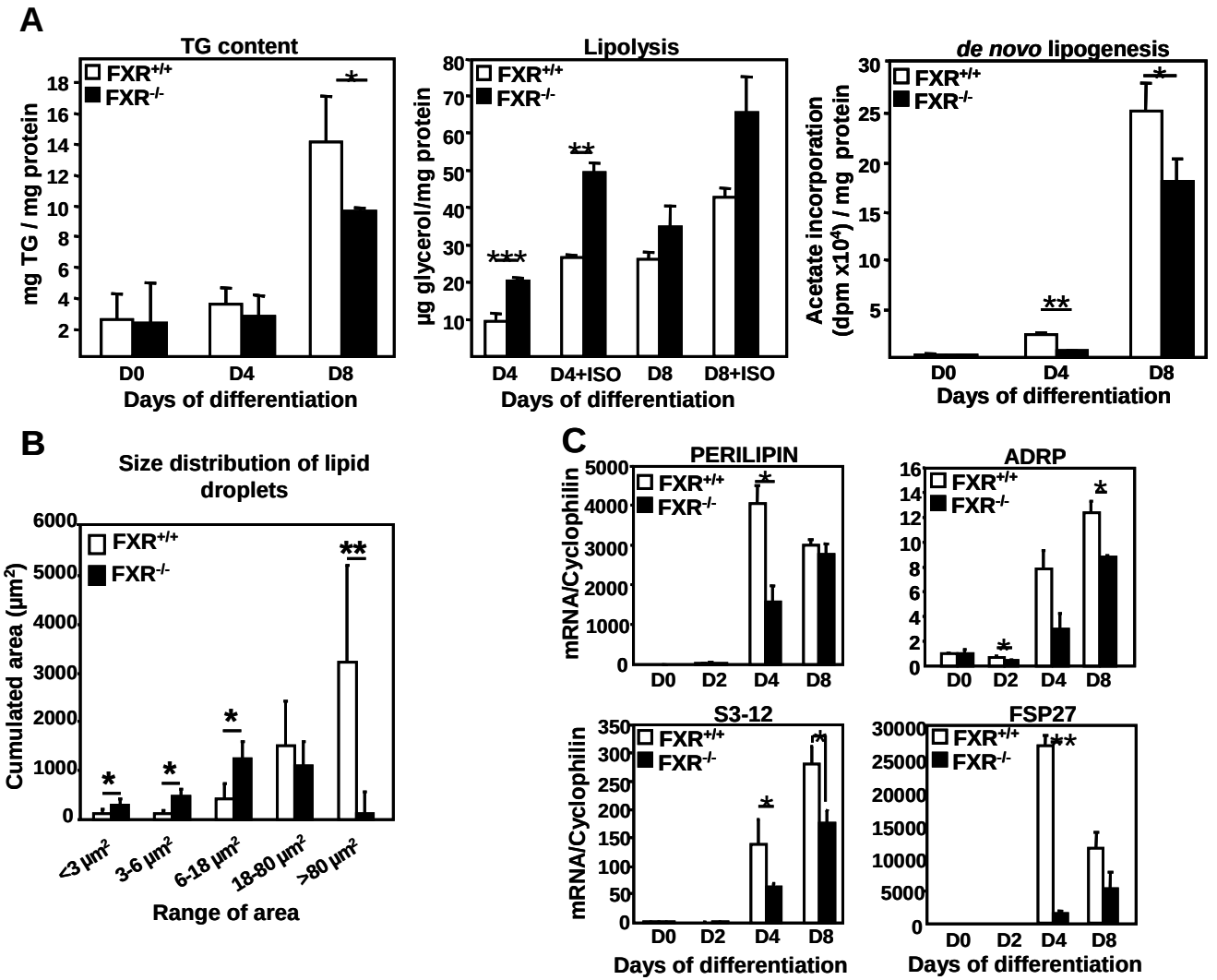

Abdelkarim M et *al*.. Figure 4

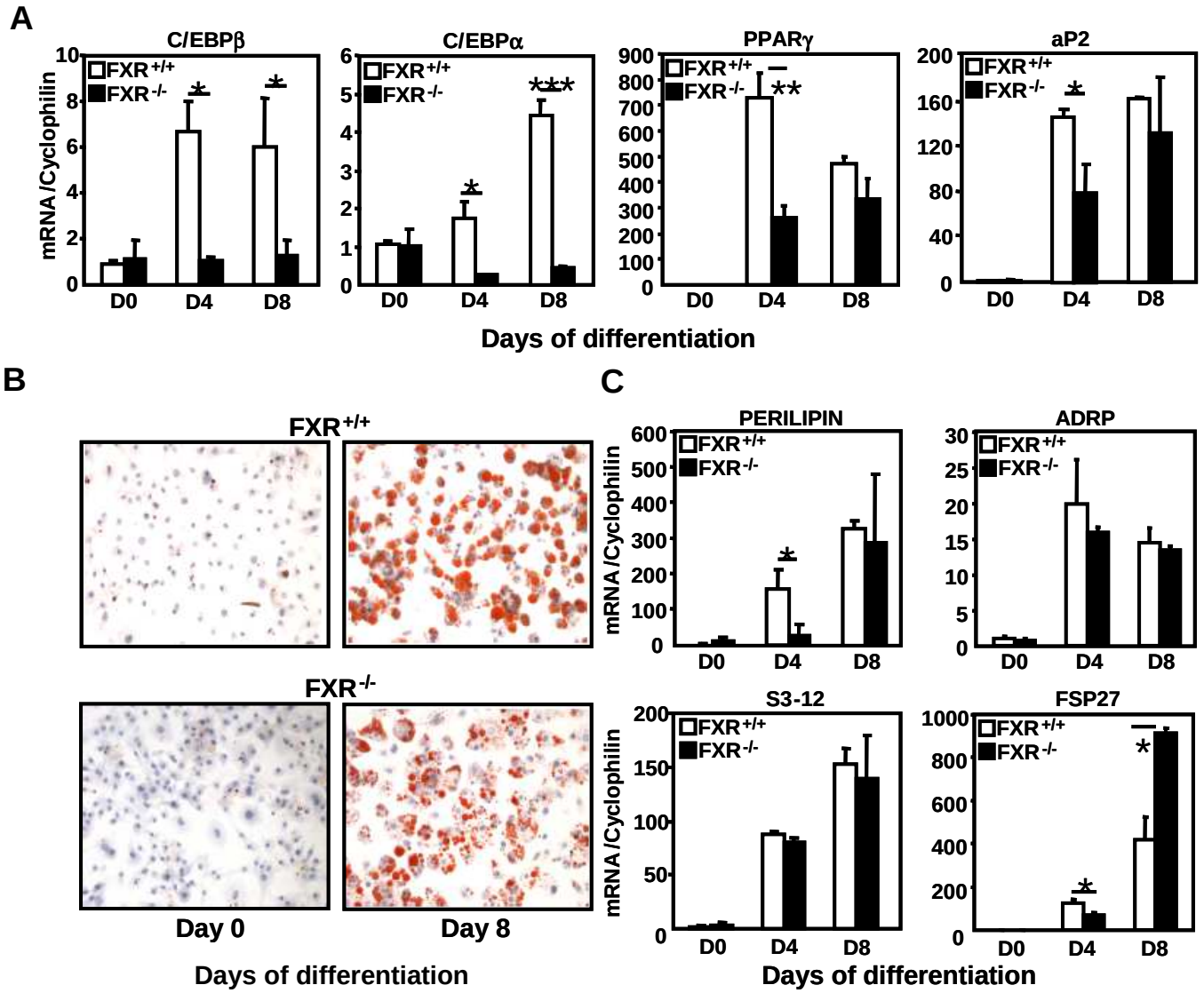

Abdelkarim M et *al*.. Figure 5

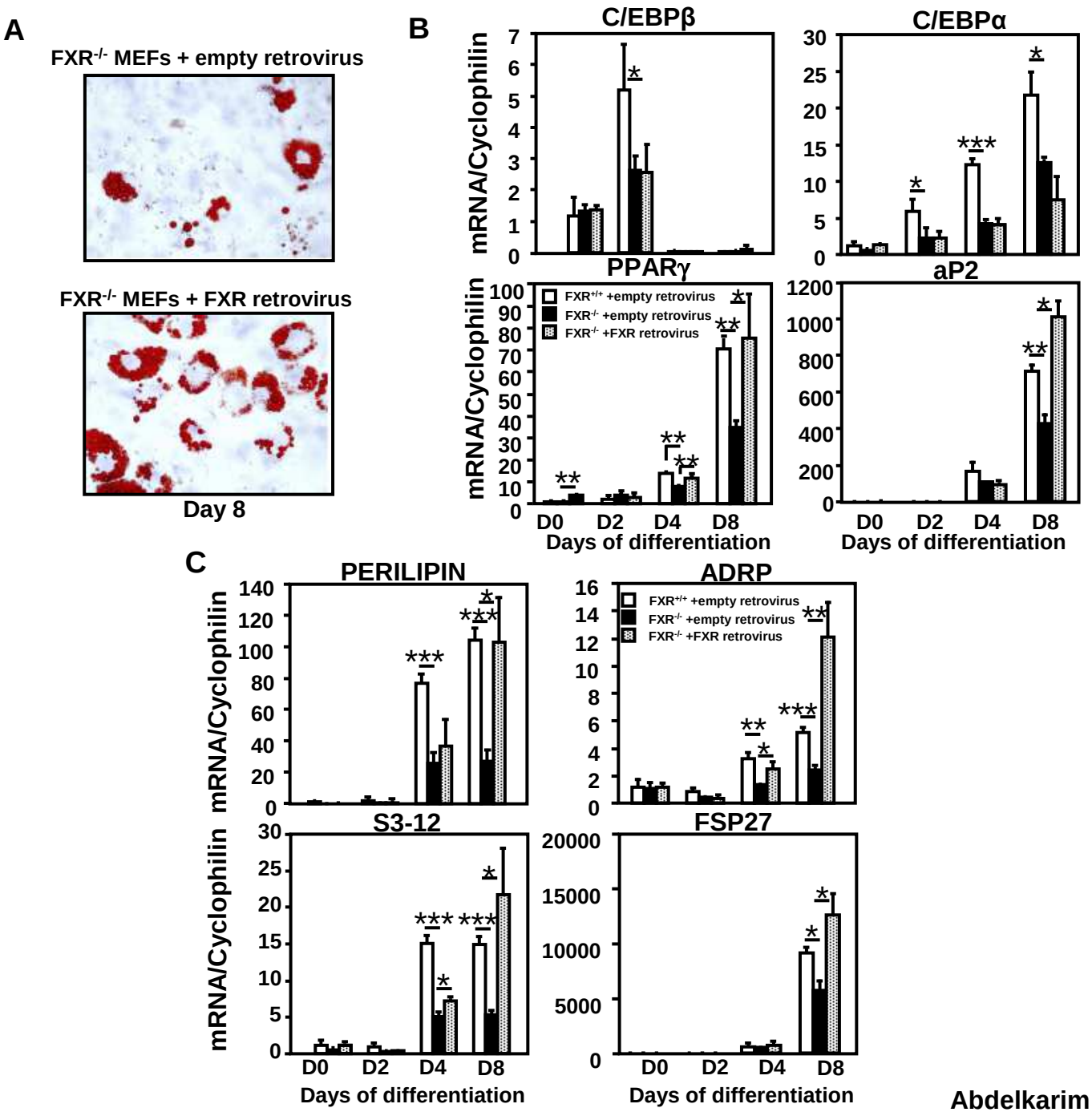

Abdelkarim M et *al*.. Figure 6

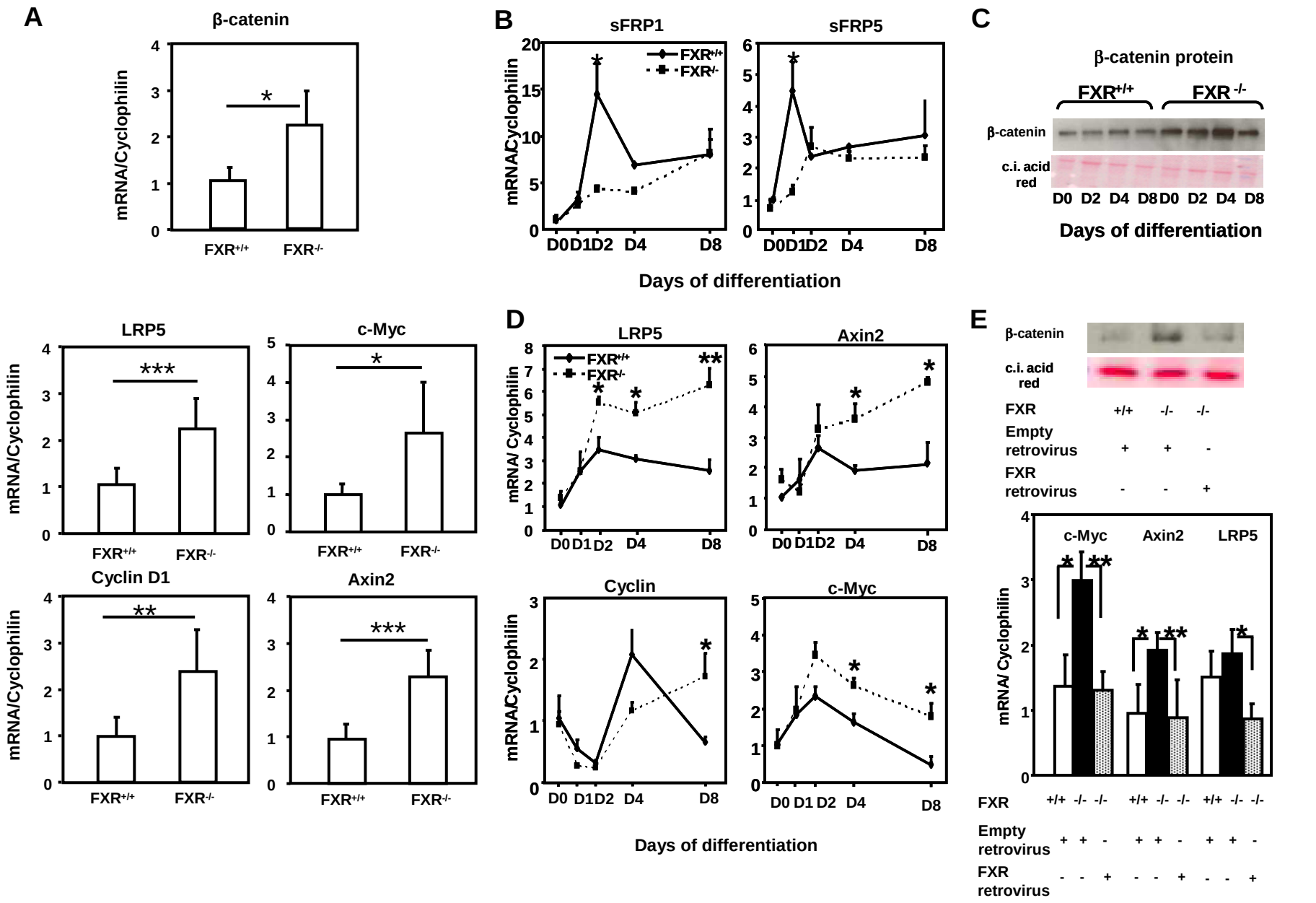

Abdelkarim M et *al*.. Figure 7

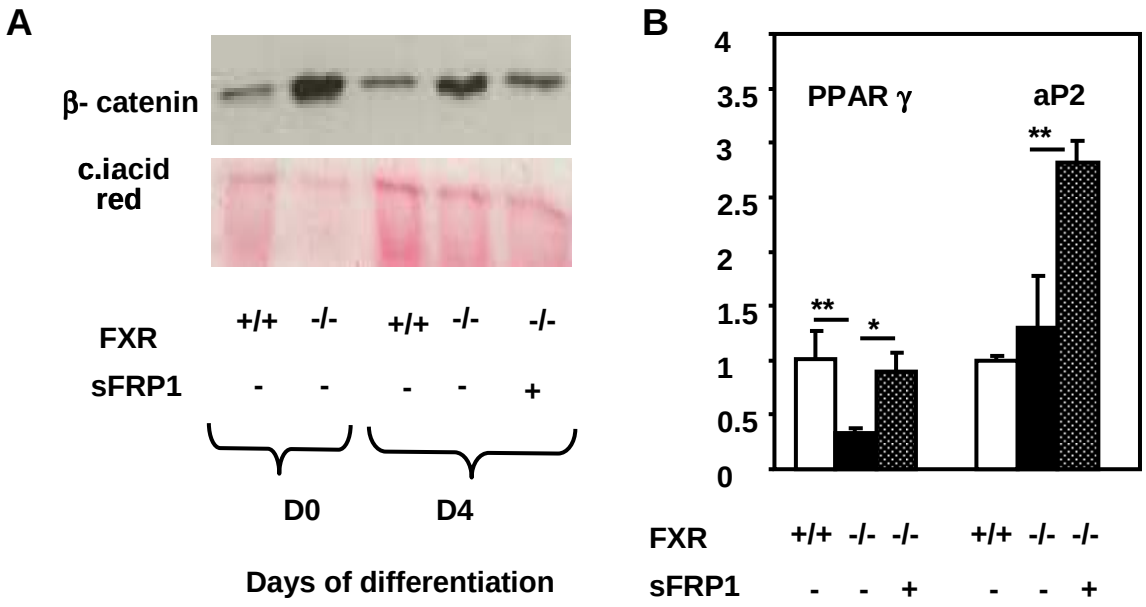

Abdelkarim M et *al*.. Figure 8

The farnesoid X receptor regulates adipocyte differentiation and function by promoting peroxisome proliferator-activated receptor-gamma and interfering with the WNT/ β catenin pathways

Mouaadh Abdelkarim, Sandrine Caron, Christian Duhem, Janne Prawitt, Julie Dumont, Anthony Lucas, Emmanuel Bouchaert, Olivier Briand, John Brozek, Folkert Kuipers, Catherine Fievet, Bertrand Cariou and Bart Staels

J. Biol. Chem. published online September 17, 2010 originally published online September 17, 2010
